Please cite this article in press as: He et al., Bi-allelic Loss-of-function Variants in *CFAP58* Cause Flagellar Axoneme and Mitochondrial Sheath Defects and Asthenoteratozoosperm..., The American Journal of Human Genetics (2020), https://doi.org/10.1016/j.ajhg.2020.07.010

ARTICLE

Bi-allelic Loss-of-function Variants in *CFAP58* Cause Flagellar Axoneme and Mitochondrial Sheath Defects and Asthenoteratozoospermia in Humans and Mice

Xiaojin He,[1,2,3,13] Chunyu Liu,[4,5,6,13] Xiaoyu Yang,[7,13] Mingrong Lv,[1,2,3,13] Xiaoqing Ni,[1,2,3,13] Qiang Li,[1,2,3,13] Huiru Cheng,[1,8,9] Wangjie Liu,[4,5,6] Shixiong Tian,[4,5] Huan Wu,[1,2,3] Yang Gao,[1,2,3] Chenyu Yang,[10] Qing Tan,[1,11] Jiangshan Cong,[4,5] Dongdong Tang,[1,2,3] Jingjing Zhang,[1,2,3] Bing Song,[1,2,3] Yading Zhong,[12] Hang Li,[1,11] Weiwei Zhi,[1,11] Xiaohong Mao,[1,11] Feifei Fu,[1,11] Lei Ge,[1,11] Qunshan Shen,[1,8,9] Manyu Zhang,[1,8,9] Hexige Saiyin,[4] Li Jin,[4] Yuping Xu,[1,2,3] Ping Zhou,[1,2,3] Zhaolian Wei,[1,2,3] Feng Zhang,[4,5,6,*] and Yunxia Cao[1,2,3,*]

Summary

Multiple morphological abnormalities of the sperm flagella (MMAF) is a severe form of asthenoteratozoospermia. Although recent studies have revealed several MMAF-associated genes and demonstrated MMAF to be a genetically heterogeneous disease, at least one-third of the cases are still not well understood for their etiology. Here, we identified bi-allelic loss-of-function variants in *CFAP58* by using whole-exome sequencing in five (5.6%) unrelated individuals from a cohort of 90 MMAF-affected Chinese men. Each of the men harboring bi-allelic *CFAP58* variants presented typical MMAF phenotypes. Transmission electron microscopy demonstrated striking flagellar defects with axonemal and mitochondrial sheath malformations. *CFAP58* is predominantly expressed in the testis and encodes a cilia- and flagella-associated protein. Immunofluorescence assays showed that CFAP58 localized at the entire flagella of control sperm and predominantly concentrated in the mid-piece. Immunoblotting and immunofluorescence assays showed that the abundances of axoneme ultrastructure markers SPAG6 and SPEF2 and a mitochondrial sheath protein, HSP60, were significantly reduced in the spermatozoa from men harboring bi-allelic *CFAP58* variants. We generated *Cfap58*-knockout mice via CRISPR/Cas9 technology. The male mice were infertile and presented with severe flagellar defects, consistent with the sperm phenotypes in MMAF-affected men. Overall, our findings in humans and mice strongly suggest that CFAP58 plays a vital role in sperm flagellogenesis and demonstrate that bi-allelic loss-of-function variants in *CFAP58* can cause axoneme and peri-axoneme malformations leading to male infertility. This study provides crucial insights for understanding and counseling of MMAF-associated asthenoteratozoospermia.

Introduction

Infertility, affecting tens of millions of people around the world, has become a major human health concern. Male infertility accounts for approximately half of infertile couples and can bring about severe physiological and psychological consequences.[1] Asthenoteratozoospermia, one of the main causes of male infertility (~19% of infertile men[2,3]), refers to the lack or decrease of motile sperm in the ejaculation.

Multiple morphological abnormalities of the sperm flagella (MMAF) is a subtype of asthenoteratozoospermia and is characterized by abnormal flagellar phenotypes (e.g., absent, short, coiled, bent flagellar, and/or irregular caliber) and severe impairment of sperm motility. In the first report of MMAF,[4] bi-allelic *DNAH1* (MIM: 603332) variants were identified as the genetic cause. Now, eighteen genes are known to be associated with MMAF via different pathogenic mechanisms. For example, bi-allelic variants in *CFAP43* (MIM: 617558), *CFAP44* (MIM: 617559), *CFAP65* (MIM: 614270), *CFAP251* (MIM: 618146), *DNAH1*, and *DNAH17* (MIM: 610063) can cause structural defects of the axoneme.[4–11] Furthermore, bi-allelic variants in *FSIP2* (MIM: 618153) are associated with a complete disorganization of the fibrous sheath, which in turn may lead to defects in the axoneme.[12,13] Additionally, bi-allelic variants in *CFAP69* (MIM: 617949), *TTC21A* (MIM: 618429), and *TTC29* (MIM: 618735) can impair the molecular motor-driven intra-manchette transport (IMT) and intra-flagellar transport (IFT) process during assembly of the cilia and

[1]Reproductive Medicine Center, Department of Obstetrics and Gynecology, the First Affiliated Hospital of Anhui Medical University, Hefei 230022, China; [2]NHC Key Laboratory of Study on Abnormal Gametes and Reproductive Tract (Anhui Medical University), Hefei 230032, China; [3]Key Laboratory of Population Health Across Life Cycle (Anhui Medical University), Ministry of Education of the People's Republic of China, Hefei 230032, China; [4]Obstetrics and Gynecology Hospital, NHC Key Laboratory of Reproduction Regulation (Shanghai Institute of Planned Parenthood Research), State Key Laboratory of Genetic Engineering at School of Life Sciences, Fudan University, Shanghai 200011, China; [5]Shanghai Key Laboratory of Female Reproductive Endocrine Related Diseases, Shanghai 200011, China; [6]State Key Laboratory of Reproductive Medicine, Center for Global Health, School of Public Health, Nanjing Medical University, Nanjing 211166, China; [7]State Key Laboratory of Reproductive Medicine, Clinical Center of Reproductive Medicine, the First Affiliated Hospital of Nanjing Medical University, Nanjing 210029, China; [8]Anhui Province Key Laboratory of Reproductive Health and Genetics, Hefei 230032, China; [9]Biopreservation and Artificial Organs, Anhui Provincial Engineering Research Center, Anhui Medical University, Hefei 230032, China; [10]Center of Cryo-Electron Microscopy, Zhejiang University, Hangzhou 310058, China; [11]Anhui Provincial Human Sperm Bank, the First Affiliated Hospital of Anhui Medical University, Hefei 230022, China; [12]Department of Radiology, the First Affiliated Hospital of Anhui Medical University, Hefei 230022, China
[13]These authors contributed equally to this work
*Correspondence: zhangfeng@fudan.edu.cn (F.Z.), caoyunxia6@126.com (Y.C.)
https://doi.org/10.1016/j.ajhg.2020.07.010.

flagella, leading to failed microtubule assembly and severe defects in the axoneme.[14–18] Moreover, bi-allelic variants in *DZIP1* (MIM: 608671) can cause severe flagella defects due to abnormal centriole assembly.[19] However, only 60% of the MMAF-affected individuals have been genetically explained, and additional flagellogenesis-associated gene variants could be involved in MMAF.

In this study, we conducted whole-exome sequencing (WES) and genetic analyses in a cohort of 90 MMAF-affected Chinese men. Interestingly, bi-allelic loss-of-function (LoF) variants of *CFAP58* were found in five unrelated individuals, three of whom were from consanguineous families and the other two of whom were simplex individuals. Men harboring bi-allelic *CFAP58* variants present typical MMAF phenotypes, and transmission electron microscopy (TEM) demonstrated striking flagellar ultrastructure defects, including absence of central and/or peripheral microtubules, and malformations of the mitochondrial sheath. In addition, *Cfap58*-knockout (KO) male mice also showed typical MMAF characteristics, including severely decreased sperm motility and abnormal flagellar morphology. These findings strongly suggested that bi-allelic LoF variants of *CFAP58* can induce asthenoteratozoospermia and male infertility in humans and mice.

Material and Methods

Subjects and Clinical Investigation

A total of 90 MMAF-affected Chinese men were enrolled from the First Affiliated Hospital of Anhui Medical University and the First Affiliated Hospital of Nanjing Medical University in China. All 90 men had primary infertility for more than one year. Subjects with obvious primary ciliary dyskinesia related symptoms, such as bronchitis, sinusitis, otitis media, or pneumonia, were excluded. All individuals had normal somatic karyotypes (46, XY) with no Y chromosome microdeletions. Peripheral whole blood samples from these men were collected for subsequent genetic analysis. This study was approved by the ethics committees of the First Affiliated Hospital of Anhui Medical University and the First Affiliated Hospital of Nanjing Medical University. Informed consent was obtained from all of the subjects and their family members, as well as from the fertile control male subjects.

Semen Parameters and Sperm Morphological Analysis

Fresh semen samples from MMAF-affected men and male control subjects were collected and examined in the source laboratories during routine biological examination of the individuals in accordance with the World Health Organization (WHO) guidelines (5^{th} Edition).[20] Semen samples from men harboring bi-allelic *CFAP58* variants (subjects A050 IV-1, A064 II-1, N010 IV-1, and N015 II-1) were collected via masturbation after 3–7 days of sexual abstinence and evaluated after liquefaction for 30 min at 37°C. Analyses of semen volume, sperm concentration, and motility were carried out and replicated in the source hospitals during routine examination. Sperm morphology was analyzed by hematoxylin and eosin (H&E) staining and scanning electron microscopy (SEM) assays. For each subject, we examined at least 200 spermatozoa to evaluate the percentages of morphologically abnormal spermatozoa.

The semen samples of adult male mice were obtained from the cauda epididymis and diluted for 15 min at 37°C with 1 mL solution of capacitation. The parameters of semen were further analyzed by a computer-assisted analysis system. At least three male C57BL/6J mice that were 8 weeks of age were analyzed in each group.

WES, Bioinformatic Analysis, and Sanger Sequencing

Genomic DNA was extracted from whole peripheral blood for WES. The human exome was enriched by the SureSelect XT Human All Exon Kit (Agilent) and then sequenced with the Illumina HiSeq X-TEN platform. The original data were mapped to the human genome assembly GRCh37/hg19 by the Burrows-Wheeler Aligner (BWA) software.[21] We employed the Picard software to remove PCR duplicates and evaluate the quality of variants by attaining effective reads, effective base, average coverage depth, and 90–120× coverage ratio. Details on the methods used for analysis were described previously.[19] *CFAP58* variants identified by WES were further validated by Sanger sequencing. PCR primers and protocols used for each *CFAP58* variant are listed in Table S1.

Scanning and Transmission Electron Microscopy

For SEM and TEM, spermatozoa were prepared in accordance with the protocol described previously.[17] For SEM, the samples were subsequently dehydrated in a series of ethanol dilutions at increasing concentrations and dried with hexamethyldisilazane (HMDS). Samples were then air-dried, added dropwise to the specimen stubs, sputter coated, and examined via field emission SEM (Nova Nano 450, Thermo Fisher). For TEM, the samples were subsequently fixed with 1% osmium tetroxide and dehydrated with graded ethanol (50%, 70%, 90%, and 100%) and 100% acetone. After they were infiltrated with acetone and SPI-Chem resin and embedded with Epon 812, the samples were sliced by ultra-microtome and stained by uranyl acetate and lead citrate. Cryo-electron microscopy (TecnaiG2 Spirit 120 kV) was used for observation and photography.

Reverse Transcription PCR and Quantitative Real-Time PCR

Total RNA of adult mouse tissues was extracted with the TRIzol Reagent (Invitrogen) and converted into cDNAs via the PrimeScript RT Reagent Kit (Takara). The obtained cDNAs were used for subsequent real-time fluorescence quantitative PCR analysis with the LightCycler 480 SYBR Green I Master (Roche). mRNA expression was quantified according to the $2^{-\Delta\Delta Ct}$ method. *Gapdh* was used as an internal control. PCR primers are presented in Table S2.

Immunoblotting

Human sperm and mouse testis samples were homogenized in 200 μL radioimmunoprecipitation assay (RIPA) buffer (Beyotime) via an ultrasonic homogenizer and then heated at 100°C for 15 min. The lysates were separated on 10% polyacrylamide gel by SDS-PAGE and transferred to PVDF (polyvinylidene fluoride) membrane. Then the membrane was sealed for 1 h at 25°C with 5% milk diluted with TBST (TBS-0.1% Tween-20). Anti-CFAP58 antibody (PA5-57714, Invitrogen or PA5-65174, Invitrogen), anti-HSP60 antibody (ab13532, Abcam), and anti-SPEF2 antibody (HPA040343, Sigma) were diluted in TBST at 1:1,000 and incubated with the membranes at 4°C overnight. Enhanced chemiluminescence (ECL) (BL520A, Biosharp) was used for visualization. The reference protein β-tubulin was used as a loading control.

Immunofluorescence Assays

We preprocessed spermatozoa samples by following previously published procedures[19] and incubated them overnight at 4°C with the following primary antibodies: rabbit polyclonal anti-CFAP58 (PA5-65174, Invitrogen, 1:100), rabbit polyclonal anti-SPAG6 (HPA038440, Sigma, 1:100), rabbit polyclonal anti-SPEF2 (HPA040343, Sigma, 1:100), mouse polyclonal anti-HSP60 (ab13532, Abcam, 1:100), mouse monoclonal anti-acetylated alpha-tubulin (T6793, Sigma, 1:500), and rabbit anti-acetylated alpha-tubulin (mAb#5335, Cell Signaling Technology, 1:500). Washes were performed with phosphate buffer saline (PBS) followed by 1 h of incubation at 25°C with highly cross-adsorbed secondary antibodies at a dilution of 1:500. The antibodies employed in this analysis were as follows: anti-rabbit-Alexa Fluor-594 for anti-CFAP58, anti-SPAG6, and anti-SPEF2 and anti-mouse-Alexa Fluor-488 for anti-HSP60 and anti-acetylated alpha-tubulin. Images were captured with an LSM 800 confocal microscope (Carl Zeiss AG).

Generation of the *Cfap58*-KO Mouse Model

The generation of a KO mouse model harboring the frameshift variant in *Cfap58* (NCBI: NM_001163267.1) was performed with CRISPR-Cas9 technology.[17,19] Two single-guide RNAs (sgRNAs) were designed for *Cfap58* exon 10 (Table S3). A frameshift variant in *Cfap58* was identified by Sanger sequencing in the founder mouse and its offspring (the primer information is provided in Table S4). All experiments involving mice were performed according to the US National Institutes of Health's Guide for the Care and Use of Laboratory Animals. This study was approved by the animal ethics committee of Anhui Medical University. Adult mice (aged 8 weeks or older) were selected for subsequent experiments.

Mouse Tissue Histology

Fresh mouse testes were fixed with modified Davidson's solution (50% diluted water, 30% formaldehyde, 15% ethanol, and 5% glacial acetic acid) for more than 48 h. After fixation, the tissue was dehydrated in gradient ethanol (70% ethanol for 24 h, 80% ethanol for 2 h, 90% ethanol for 2 h, and 100% ethanol for 1 h). Then the tissues were placed in xylene for 1 h and finally embedded in paraffin wax and sectioned to ~4 μm. For H&E staining, sections were deparaffinized in xylene at 65°C overnight. Then the slides were stained, dehydrated, and mounted.

Mating Test

Fertility was investigated in wild-type (WT) and *Cfap58*-KO adult male mice. At least three male mice that were 8–12 weeks of age were analyzed in each group. Each male mouse and two WT C57BL/6J females (8–12 weeks of age) were caged. Vaginal plugs were checked every morning. Once a vaginal plug was identified, the male mouse was allowed to rest for 2 days before another two females were placed in the cage. After mating, the female mice were separated and fed in a single cage and the pregnancy results and number of pups were recorded.

Results

Identification of Bi-allelic LoF Variants of *CFAP58* in Men with MMAF

According to our established protocol, WES and bioinformatic analysis were performed in a cohort of 90 MMAF-affected men.[17] We identified five unrelated individuals with bi-allelic LoF variants in *CFAP58* (NCBI: NM_001008723.2), accounting for 5.6% (5/90) of the cohort (Figure 1A). *CFAP58* (cilia- and flagella-associated protein 58) encodes a predicted 872-amino-acid protein that comprises two coiled-coil (CC) domains (Figure 1B). According to the EMBL-EBI Expression Atlas and the NCBI and GTEx databases, *CFAP58* is preferentially expressed in human testis. Quantitative real-time PCR analysis in adult mouse tissues also revealed that *Cfap58* mRNA was predominantly expressed in the testis (Figure S1).

In two consanguineous families (A050 and N011) and one non-consanguineous family (N015), homozygous *CFAP58* stop-gain variants c.2092C>T (p.Arg698*), c.1696C>T (p.Gln566*), and c.2274C>A (p.Tyr758*) were identified in probands A050 IV-1, N011 IV-1, and N015 II-1, respectively. These variants were inherited from their heterozygous parental carriers (Figure 1A) but are very rare in the general human population (Table 1). Each *CFAP58* stop-gain variant introduces a premature stop codon and thus is expected to produce either no protein or truncated non-functional proteins.

We also identified an additional subject, A064 II-1, harboring compound heterozygous variants of *CFAP58* (c. 2092C>T [p. Arg698*], c.1429del [p.lle477*]). Sanger sequencing confirmed that these two variants were also inherited from the subject's heterozygous parental carriers. Notably, public genome data from the 1000 Genomes Project database and gnomAD indicated that these two truncating variants were found at very low allele frequencies (ranging from 0 to 6.5×10^{-5}) in the general population. Furthermore, a homozygous frameshift variant in *CFAP58* (c.2052del [p.His685Thrfs*7]) was identified in proband IV-1 from consanguineous family N010 (Figure 1A). This frameshift variant is absent in the 1000 Genomes Project database and gnomAD (Table 1). Each of the five aforementioned truncating variants are located at the CC domains of CFAP58 and are thus expected to damage the CC domains (Figure 1B).

Asthenoteratozoospermia Phenotypes in Men Harboring Bi-allelic *CFAP58* Variants

Based on WHO guidelines, sperm concentrations were either normal or slightly decreased in five men harboring bi-allelic *CFAP58* variants. However, the progressive motility rates in four of these five affected individuals dramatically decreased to zero, and the remaining affected individual had a progressive motility rate of only 2.1% (Table 2). The morphology of the sperm cells was assessed with H&E staining. Compared with the long and smooth flagella in the normal spermatozoa from a fertile male control individual, the spermatozoa from men harboring bi-allelic *CFAP58* variants displayed obvious MMAF phenotypes, including short, coiled, absent, and irregular-caliber flagella (Figure 2A and Figure S2). More than 94% of the spermatozoa from men harboring bi-allelic *CFAP58* variants

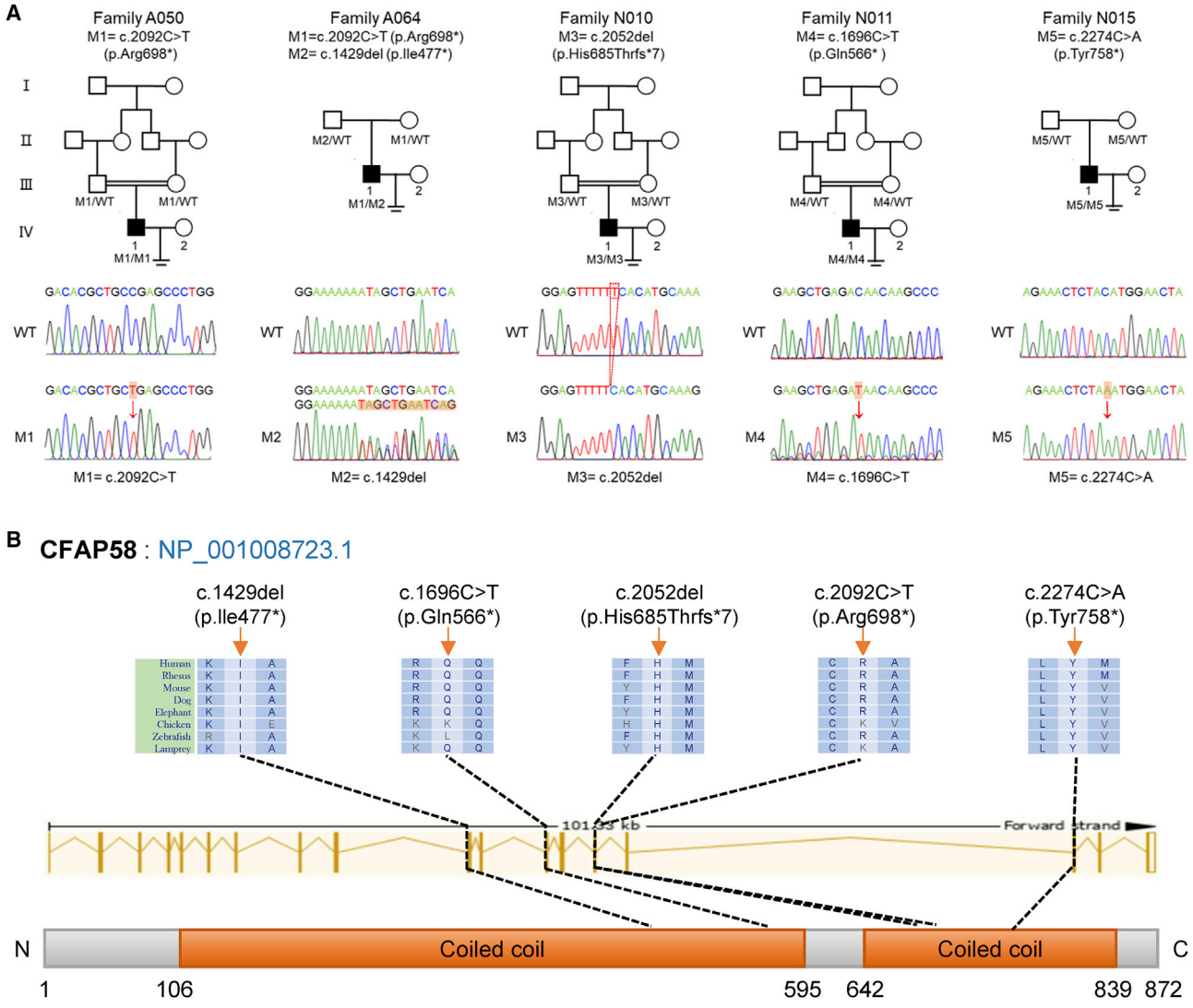

Figure 1. Identification of Bi-allelic *CFAP58* Variants in MMAF-affected Men

(A) Pedigree analysis of the five families affected by bi-allelic *CFAP58* variants that were identified by WES. Black filled squares indicate infertile men in these families. Sanger sequencing results are shown under the pedigrees. The mutated positions are indicated by red arrows and boxes.

(B) Schematic representation of the domains of CFAP58 protein product. The positions of the novel or rare *CFAP58* variants identified in this study are indicated by black dotted lines. Sequence alignment shows conservation of the mutated residues among different species. Orange squares stand for the typical protein-folding motif called coiled-coil (CC) domains according to the NCBI browser.

displayed abnormal flagella in which the major flagellar abnormalities were coiled and short flagella (Table 2).

To investigate the pathogenicity of the identified *CFAP58* LoF variants, we examined the localization and abundance of CFAP58 in sperm cells from a control individual and men harboring bi-allelic *CFAP58* variants by using a commercial antibody against CFAP58. By immunofluorescence staining, we found that CFAP58 localized at the entire flagella in the fertile control individual and strongly concentrated at the mid-piece (Figure 2B). However, CFAP58 staining was almost absent in the sperm flagella of subjects A050 IV-1, A064 II-1, and N015 II-1 (Figure 2B). Immunoblotting analysis was performed with the spermatozoa from men harboring bi-allelic *CFAP58* variants (except subject N011 IV-1, whose semen was not sufficient). We found that CFAP58 was almost absent in the samples of men harboring bi-allelic *CFAP58* variants (Figure 2C), which could be caused by the nonsense-mediated mRNA decay triggered by premature translation termination. These experimental results reveal that CFAP58 deficiency due to bi-allelic LoF variants of *CFAP58* can cause MMAF-related asthenoteratozoospermia.

CFAP58 Deficiency Associated with Axoneme and Mitochondrial Sheath Malformations

Axoneme, the core of motile cilia and flagella, is a highly evolutionarily conserved "9 + 2" structure, which consists of nine doublets of microtubules (DMTs) circularly arranged around a central pair of microtubules (CP). In addition, the sperm flagellum harbors specific peri-axonemal

Table 1. Bi-allelic Variants of *CFAP58* Identified in MMAF-Affected Subjects

	***CFAP58* Variants**				**Allele Frequency in Population**	
Subjects	**cDNA Mutation**	**Protein Alteration**	**Mutation Type**	**Affected Allele**	**1KGP**	**gnomAD**
A050 IV-1	c.2092C>T	p.Arg698*	stop-gain	homozygous	0	0.000065
A064 II-1	c.1429del	p.lle477*	frameshift	heterozygous	0	0.000021
	c.2092C>T	p.Arg698*	stop-gain	heterozygous	0	0.000065
N010 IV-1	c.2052del	p.His685Thrfs*7	frameshift	homozygous	0	0
N011 IV-1	c.1696C>T	p.Gln566*	stop-gain	homozygous	0	0.0000020
N015 II-1	c.2274C>A	p.Tyr758*	stop-gain	homozygous	0	0

NCBI accession number of CFAP58 is NM_001008723.2. Abbreviations are as follows: 1KGP, 1000 Genomes Project; gnomAD, the Genome Aggregation Database.

structures, including a helical mitochondrial sheath in the mid-piece, a fibrous sheath in the principal piece, and outer dense fibers (ODFs) in the mid-piece and the proximal part of the principal piece (Figure 3A). We performed TEM analysis to investigate the sperm flagellar ultrastructure of men harboring bi-allelic *CFAP58* variants, and cross-sections of the sperm flagella revealed various axonemal malformations, including absence of CP ("9 + 0" or "9 + 1"), absence of DMTs, and the complicated disorganization of the "9 + 2" structure (Figure 3A). We observed 118, 101, 79, and 100 cross-sections from a control individual and three affected subjects, A050 IV-1, A064 II-1, and N015 II-1, respectively. Cross-section quantification indicated that more than 90% of the axonemal cross-sections were abnormal in men harboring bi-allelic *CFAP58* variants, which was much higher than that of the control individual. The main defective types were absence of CP (12.9%, 57.0%, and 76.0% for subjects A050 IV-1, A064 II-1, and N015 II-1, respectively) and absence of DMTs (41.6%, 24.1%, and 9.0% for subjects A050 IV-1, A064 II-1, and N015 II-1, respectively). The residual fraction of defects presented with complicated axonemal disorganization of CP, DMTs, nexin, dynein arms, mitochondrial sheath, and/or ODFs (Figure 3B). In addition, we found that the number of ODFs was almost doubled in some of the flagellar mid-piece from subjects A050 IV-1 and A064 II-1 (Figure 3A). Intriguingly, immunofluorescence analysis also revealed an increased staining of ODF2 at the shortened and coiled flagella in the spermatozoa of men harboring bi-allelic *CFAP58* variants (Figure S3), which might indicate the important role of CFAP58 in ODF protein transportation.

To further investigate the ultrastructural defects evidenced by TEM, SPAG6, a marker of the central pair microtubules, was examined in the sperm from a control individual and men harboring bi-allelic *CFAP58* variants. Immunofluorescence assay revealed that SPAG6 was located at the entire flagellum in the control sperm, which is consistent with the localization of CFAP58 (Figure 3C). On the contrary, SPAG6 was almost absent in the short or coiled flagella of men harboring bi-allelic *CFAP58* variants (subjects A050 IV-1, A064 II-1, and N015 II-1) (Figure 3C). In addition, we also examined the localization and abundance of SPEF2, a protein required for sperm flagellar assembly.[23,24] Compared with the obvious staining in the spermatozoa from a control individual, SPEF2 was almost absent or dramatically decreased in the sperm flagella of men harboring bi-allelic *CFAP58* variants (Figure 3D). The deficiencies of SPAG6 and SPEF2 in CFAP58-affected flagella strongly suggested the defects of CP and DMTs in the spermatozoa from men harboring bi-allelic *CFAP58* variants.

To confirm the universality of SPAG6 and SPEF2 decay in the CFAP58-deficient sperm, we also performed immunoblotting with 20×10^6 spermatozoa from men harboring bi-allelic *CFAP58* variants. Both SPAG6 and SPEF2 were absent in the sample of subject A064 II-1 and obviously decreased in those of subjects A050 IV-1, N010 IV-1, and N015 II-1 (Figure 3E). These findings indicated that the absences of CP and DMTs in the cross-sections under TEM were universal defects of the sperm from men harboring bi-allelic *CFAP58* variants.

Intriguingly, longitudinal sections of the flagella observed by TEM further revealed mitochondrial sheath malformations. When compared to the regularly arranged mitochondrial sheath in the control individual, the sperm of subject A050 IV-1 showed the completely disorganized mid-piece with a misshapen mitochondrial sheath, fibrous sheath, and ODFs (Figure 4A). Notably, the sperm of subject N015 II-1 displayed an abnormal flagellar assembly with a shortened mitochondrial sheath (Figure 4A). To further investigate the severity of mitochondrial sheath malformation in men harboring bi-allelic *CFAP58* variants, we conducted immunofluorescence and immunoblotting assays for HSP60, a mitochondrial chaperonin. Immunofluorescence assays with the spermatozoa from a control individual showed that HSP60 localized at the mid-piece of flagellum, which can visualize the mitochondrial sheath well (Figure 4Bi). In contrast, HSP60 was absent or significantly decreased in the sperm cells of men harboring bi-allelic *CFAP58* variants (subjects A050 IV-1, A064 II-1, and N015 II-1) (Figures 4Bii, 4Biii, and 4Biv). Immunoblotting also indicated that HSP60 was significantly decreased in the spermatozoa from men harboring bi-allelic *CFAP58*

Table 2. Semen Routine Parameters and Sperm Morphology of Men Harboring Bi-allelic *CFAP58* Variants

Subjects	A050 IV-1	A064 II-1	N010 IV-1	N011 IV-1	N015 II-1	Reference Values
Semen Parameters						
Semen volume (mL)	2.5	5.3	3.0	3.2	6.1	>1.5
Concentration (10^6/mL)	38.6	10.7[a]	10.0[a]	8.5[a]	20.0	>15.0
Motility (%)	3.9[a]	1.6[a]	6.4[a]	2.1[a]	0[a]	>40.0
Progressive motility (%)	0[a]	0[a]	0[a]	2.1[a]	0[a]	>32.0
Sperm Morphology						
Normal flagella (%)	6.1[a]	0[a]	6.0[a]	2.0[a]	0[a]	>23.0
Absent flagella (%)	13.3[a]	9.7[a]	3.0	6.0[a]	11.0[a]	<5.0
Short flagella (%)	37.9[a]	67.7[a]	83.0[a]	85.0[a]	86.0[a]	<1.0
Coiled flagella (%)	42.2[a]	22.6[a]	5.0	3.0	1.0	<17.0
Angulation (%)	0.5	0	2.0	4.0	2.0	<13.0
Irregular caliber (%)	0	0	1.0	0	0	<2.0

Lower and upper reference limits according to the World Health Organization standards[20] and the distribution ranges of morphologically abnormal spermatozoa observed in fertile individuals.[22] At least 200 spermatozoa were observed for morphology analysis.
[a]Abnormal values.

variants (Figure 4C). These findings strongly support the idea that mitochondrial sheath malformations were universal defects in the sperm cells of men harboring bi-allelic *CFAP58* variants.

Phenotypical Characterization of *Cfap58*-KO Male Mice

To further assess the impact of CFAP58 on mouse spermatogenesis and flagellogenesis, we generated *Cfap58*-KO mice by using CRISPR-Cas9 technology. A *Cfap58* frameshift variant (a 13-bp deletion plus a 3-bp insertion at the end of deletion) in exon 10 (Figure S4A), which was predicted to induce a premature translational termination (p.Asp497Lysfs*16), was generated (Figure S4B). Immunoblotting indicated that CFAP58 (indicated by a red arrow in the figure) was nearly absent in the testis of *Cfap58*-KO male mice when compared with WT male mice (Figure 5D). Our experiments revealed that *Cfap58*-KO male mice were completely infertile (Figure 5A). We also compared testis weights and sizes between WT and *Cfap58*-KO male mice, but no significant differences were found (Figures 5B and 5C).

Semen characteristics and sperm morphology were investigated with the sperm collected from the cauda epididymis of WT and *Cfap58*-KO male mice. Compared with WT male mice, sperm concentration was significantly decreased and motility rate was as low as zero in *Cfap58*-KO male mice (Figures 5E and 5F). Morphology analysis revealed that CFAP58-deficient spermatozoa were abnormal and mainly had short (50.7 ± 1.5%, n = 3) and coiled flagella (39.0 ± 3.7%, n = 3) (Figure 5G and Table 3).

Immunofluorescence assays were performed with the sperm cells from WT and *Cfap58*-KO male mice. Consistent with the findings in human sperm cells, CFAP58 localized at the entire flagella and predominantly concentrated in the mid-piece in WT male mice (Figure 5Hi). In contrast, CFAP58 was nearly absent in the sperm cells of *Cfap58*-KO male mice (Figures 5Hii and 5Hiii). These findings further suggested that *Cfap58* nonsense-mediated mRNA decay induced premature translational termination, which subsequently caused defective flagellogenesis in mice. Finally, H&E staining was performed on the testis of WT and *Cfap58*-KO male mice. In seminiferous tubules (stages VII and VIII), no obvious differences in spermatogonia, spermatocyte, and/or round spermatid were observed between WT and *Cfap58*-KO male mice, whereas elongating spermatids with smooth flagella were almost absent in *Cfap58*-KO male mice (Figure S5). Overall, the sperm phenotypes of *Cfap58*-KO male mice further indicated that CFAP58 deficiency caused severe sperm abnormalities and male infertility.

Discussion

As mentioned above, we identified bi-allelic truncating variants of *CFAP58* in five (5.6%) unrelated individuals from a cohort of 90 MMAF-affected men. The WES results revealed no other pathogenic variants of previously known MMAF-related genes in these men harboring bi-allelic *CFAP58* variants. Notably, each of these *CFAP58* variants was absent or observed at very low allele frequencies in human populations, which fits the autosomal recessive inheritance of deleterious *CFAP58* variants in MMAF. Further experiments, including immunoblotting and immunofluorescence staining, showed that CFAP58 was absent in the spermatozoa from men harboring bi-allelic *CFAP58* variants. Therefore, the MMAF phenotypes in these cases are likely to be explained by bi-allelic LoF variants in *CFAP58*.

CFAP58, also named coiled-coil domain-containing 147 (CCDC147), is an evolutionarily conserved protein

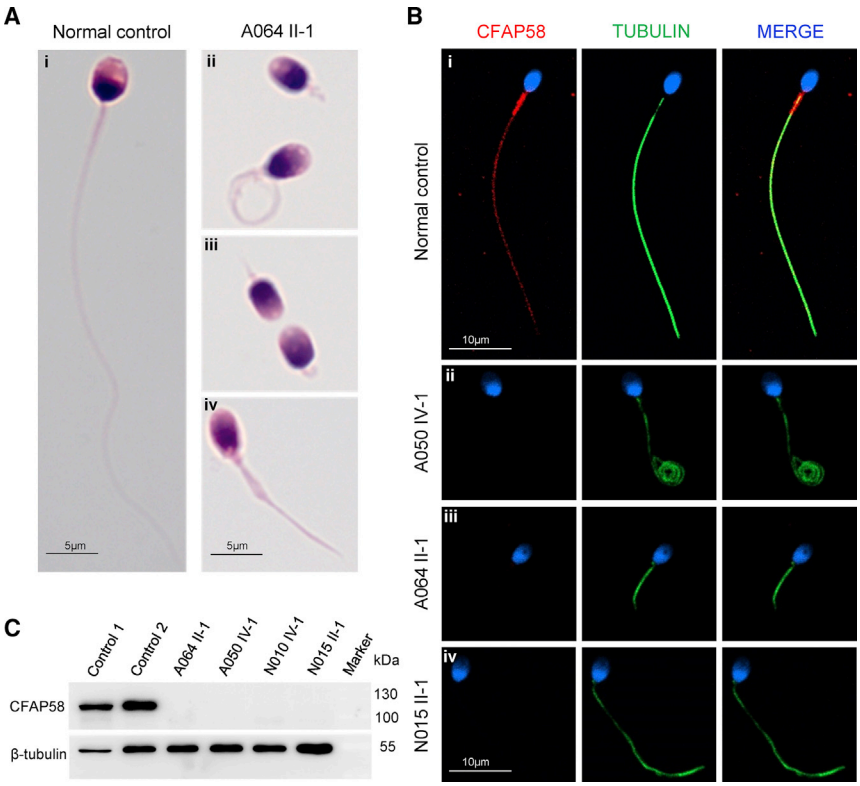

Figure 2. Morphology and CFAP58 Deficiency of the Spermatozoa from the Control Individuals and Men Harboring Bi-allelic *CFAP58* Variants

(A) The morphology of the spermatozoa from a fertile control individual (i) and subject A064 II-1 under light microscopy. Multiple images were taken, and typical features of abnormal spermatozoa are exemplified, such as coiled, absent, and short flagella (ii–iv). Scale bars: 5 μm.

(B) Immunofluorescence staining of CFAP58 in the spermatozoa from a control individual and three men harboring bi-allelic *CFAP58* variants. Anti-CFAP58 (red) and anti-α-tubulin (green) antibodies were used. The nuclei of spermatozoa were Hoechst labeled (blue). In the control individual, CFAP58 localized along the entire sperm flagella and concentrated on the mid-piece of the flagella (i). However, the CFAP58 signal is absent from the sperm flagella of men harboring bi-allelic *CFAP58* variants (ii–iv). Scale bars: 10 μm.

(C) CFAP58 abundances were analyzed by immunoblotting in the sperm from two control individuals and four men harboring bi-allelic *CFAP58* variants. β-tubulin was used as a loading control. CFAP58 was absent in the sperm samples of subjects A064 II-1, A050 IV-1, N010 VI-1, and N015 II-1.

with CC domains (Figure 1B). CC domains are built by two or more alpha-helices that wind around each other to form a supercoil.[25] Although the structure is rather simple, the CC domains represent a highly versatile protein-folding motif. CC domains can provide mechanical stability to cells, and they are also involved in movement processes. Furthermore, they can also be involved in signal-transducing events or act as a molecular recognition system. Therefore, the high versatility of the CC protein folding motif explains its widespread existence in nature.[26]

Previous studies also indicate that CC domain-containing proteins can play important roles in cilia- and flagella-associated functions. For example, the testis-enriched CCDC42 performs essential functions in connecting the sperm flagella and sperm head. *Ccdc42*-KO male mice display sperm flagellar defects and are sterile.[27,28] Furthermore, the testis-enriched CCDC172 is involved in the structural linkage between the ODF and mitochondria in the mid-piece of the sperm flagella in rat spermatozoa.[29] Moreover, the deficiencies of other CC domain-containing proteins, such as CCDC103 and CCDC65, that are widely present in multiple tissues and organs lead to the occurrence of primary ciliary dyskinesia.[30,31] In this study, each MMAF-associated truncating variant in *CFAP58* affects the CC domains of CFAP58 (Figure 1B). Immunoblotting and immunofluorescence assays consistently revealed the significant reduction of CFAP58 abundances in the spermatozoa of men harboring bi-allelic *CFAP58* variants. Therefore, it is speculated that deficiency of the CC domains contained in CFAP58 might be the cause of the flagellar defects in the MMAF-affected men.

Although several MMAF-related genes have been reported, the pathogenesis of MMAF is not yet fully understood. Sperm flagellum is mainly composed of the axoneme (a microtubule-based structure). The axoneme consists of nine DMTs, each of which has type-A and type-B microtubules, surrounding a pair of central microtubule ("9 + 2" mode).[32,33] In mammals, sperm flagella also have peri-axonemal structures, which refers to peri-axial structures of the axoneme, including the fiber sheath, mitochondrial sheath, and ODFs. Peri-axoneme is necessary for structural cohesion, energy regulation, and cell signaling.[34] According to the structure of the peri-axoneme, the sperm flagella can be divided into three main sections: the mid-piece, principal piece, and terminal piece. The mid-piece consists of the mitochondrial sheath and ODFs. The principal piece is composed of the axoneme, ODFs, and fiber sheath. The terminal piece is only composed of the axoneme without surrounding structures.[34,35] According to the previous studies, any defects involving the axoneme, peri-axoneme, protein transport, or centriole assembly might lead to malformations of the sperm flagella and subsequently result in MMAF.[36]

In this study, TEM revealed serious ultrastructure defects in both the axoneme and peri-axoneme in men harboring bi-allelic *CFAP58* variants. These affected individuals presented with axonemal malformations in more

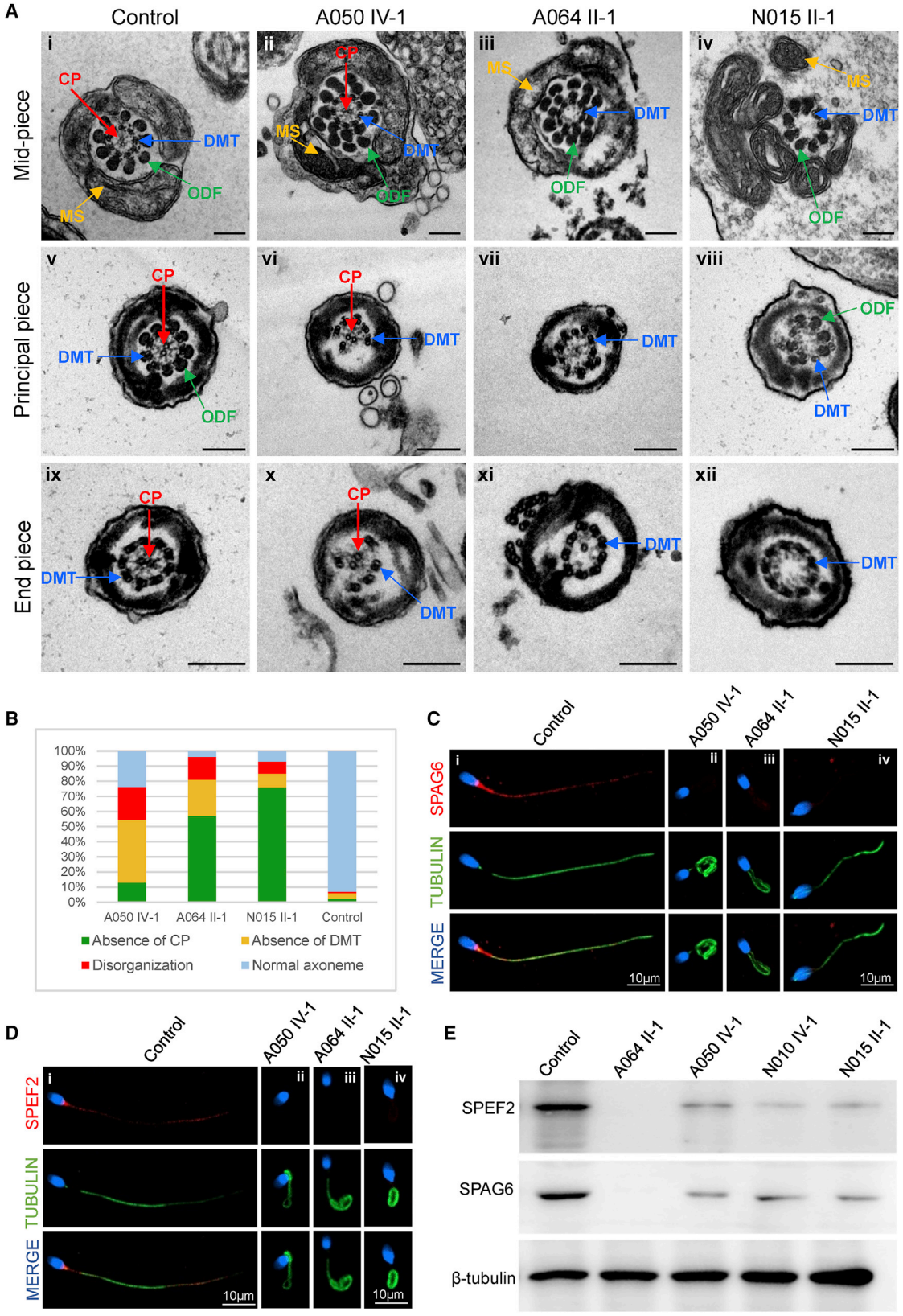

Figure 3. CFAP58 Deficiency Associated with Sperm Axonemal Malformations

(A) TEM analyses of sperm cells from a control individual and men harboring bi-allelic *CFAP58* variants. Cross-sections of the mid-piece, principal piece, and end-piece of the sperm flagella in a control man show the typical axoneme and peri-axoneme structure. The axoneme is mainly composed of "9 + 2" structure, including nine pairs of peripheral doublet microtubules (DMT; blue arrows) and the central pair of microtubules (CP; red arrows). The peri-axoneme structure includes the fiber sheath, nine outer dense fibers (ODFs; green

(legend continued on next page)

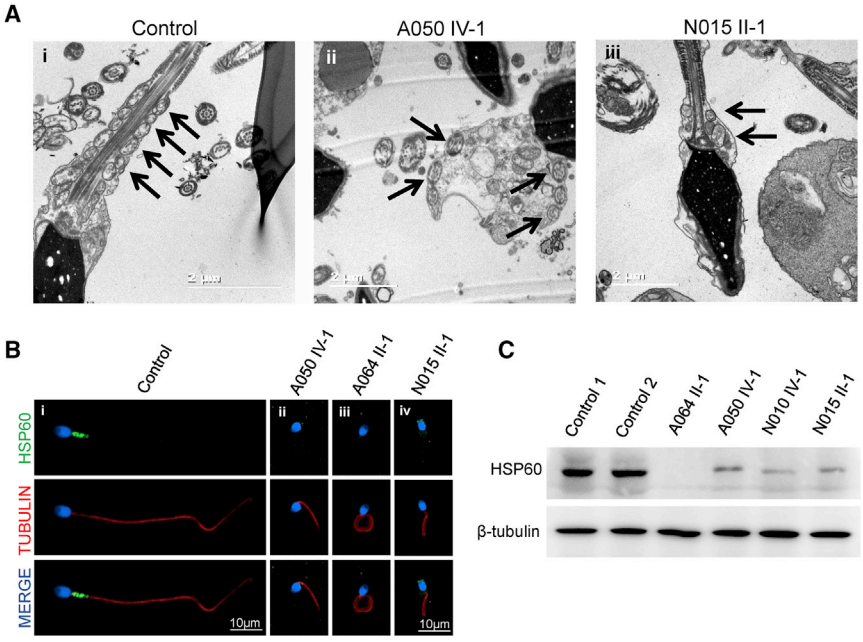

Figure 4. CFAP58 Deficiency Associated with Mitochondrial Sheath Malformations in the Sperm Flagellum

(A) The longitudinal sections of sperm flagellar mid-piece of a control individual and men harboring bi-allelic *CFAP58* variants. The normal sperm had a symmetrical mid-piece with smooth axoneme surrounding with a regularly arranged mitochondrial sheath (i). In contrast, CFAP58-deficient sperm showed a seriously disorganized mitochondrial sheath (ii and iii). Black arrows mark the mitochondrial sheath. Scale bars: 2 μm.

(B) HSP60 localization in the sperm from a control individual and men harboring bi-allelic *CFAP58* variants. HSP60 (green) localized at the flagellar mid-piece in which the mitochondrial sheath can be visualized well (i). However, HSP60 was absent or significantly decreased in the sperm from men harboring bi-allelic *CFAP58* variants (ii, iii, and iv for subjects A050 IV-1, A064 II-1, and N015 II-1). The nuclei of sperm were Hoechst labeled (blue). Anti-α-tubulin (red) marked the sperm flagella. Scale bars: 10 μm.

(C) Immunoblotting analysis was performed with the sperm cells from a control individual and men harboring bi-allelic *CFAP58* variants. The abundances of HSP60 were significantly decreased in men harboring bi-allelic *CFAP58* variants when compared with those of the control individual.

than 90% of cross-sections of the axonemes, and the main defect types were absences of CP and DMTs. SPAG6, a component of the central pair complex, is crucial for the integrity of structure and function of the axon.[37,38] SPEF2 is also widely recognized as an essential component of cilia and flagella.[23,24,39] In our study, both SPAG6 and SPEF2 dramatically decreased or were almost absent in the sperm from men harboring bi-allelic *CFAP58* variants, indicating that the absence of CP and DMTs were universal defects for *CFAP58*-associated MMAF.

In addition, there are interrelations between the axoneme and peri-axonemal structures and within peri-axonemal structures. In the mid-piece, there is an electron-dense matrix called the sub-mitochondrial reticulum between the ODF and mitochondrial sheath within peri-axonemal structures. Moreover, peri-axoneme structures attached to doublet microtubules of the axoneme through axoneme-ODF linkage.[40,41] Recently, it has been shown that mouse CFAP58 is involved in the elongation of the sperm flagellar mid-piece.[42] Here, we observed that CFAP58 predominantly concentrated in the mid-piece of the sperm flagella in both humans and mice. Severe mitochondrial sheath malformations, such as a shortened or disorganized mitochondrial sheath, were also found in the sperm cells from *CFAP58*-associated subjects. In addition, the abnormal quantities and mis-arrangements of ODFs in the mid-piece were also found in the subjects harboring bi-allelic *CFAP58* variants (Figures 3Aii and 3Aiii). It has been reported that mouse CFAP58 has a similar localization and a tight interaction with ODF2 (one of the major ODF proteins).[43] Our immunofluorescence assays also consistently indicated that ODF2 mainly localized at the mid-piece and the principal piece of control sperm flagella, but the immunofluorescence signal was obviously increased in the spermatozoa of *CFAP58*-associated subject A050 IV-1 (Figure S3). Therefore, we speculated

arrows), and a helical mitochondrial sheath (MS; yellow arrows) (i, v, and ix). Men harboring bi-allelic *CFAP58* variants suffered from various types of flagellar defects, including absence of CP (iii, iv, xi, and xii), loss of DMT (vi, viii, and x), abnormal ODF (ii, iii, iv, vii, and viii), and defective MS (iii and iv). Scale bars: 200 nm.

(B) Quantification of different categories of flagellar ultrastructural defects. Total cross-section numbers for the quantification in the control individual and men harboring bi-allelic *CFAP58* variants (subjects A050 IV-1, A064 II-1, and N015 II-1) were 118, 101, 79, and 100, respectively. Cross-sectional defects were classified into four categories: absence of CP, absence of DMT, complicated disorganization, and normal axoneme. Absences of CP and DMT were the major defect categories, which contributed to 54.5%, 81.1%, and 85.0% of the cross-sectional defects in subjects A050 IV-1, A064 II-1, and N015 II-1, respectively.

(C and D) SPAG6 and SPEF2 immunofluorescence staining of human sperm. SPAG6 (red in C) and SPEF2 (red in D) normally localized along the sperm ñagella in the control sperm. However, both SPAG6 and SPEF2 were almost absent in the sperm from men harboring bi-allelic *CFAP58* variants (subjects A050 IV-1, A064 II-1, and N015 II-1). The nuclei of spermatozoa were Hoechst labeled (blue). Anti-α-tubulin (green) marked the sperm flagella. Scale bars: 10 μm.

(E) Immunoblotting assays of SPEF2 and SPAG6 abundances. When compared with that of a control individual, the abundances of both SPEF2 and SPAG6 decreased in the sperm from men harboring bi-allelic *CFAP58* variants. Abundances were normalized with β-tubulin.

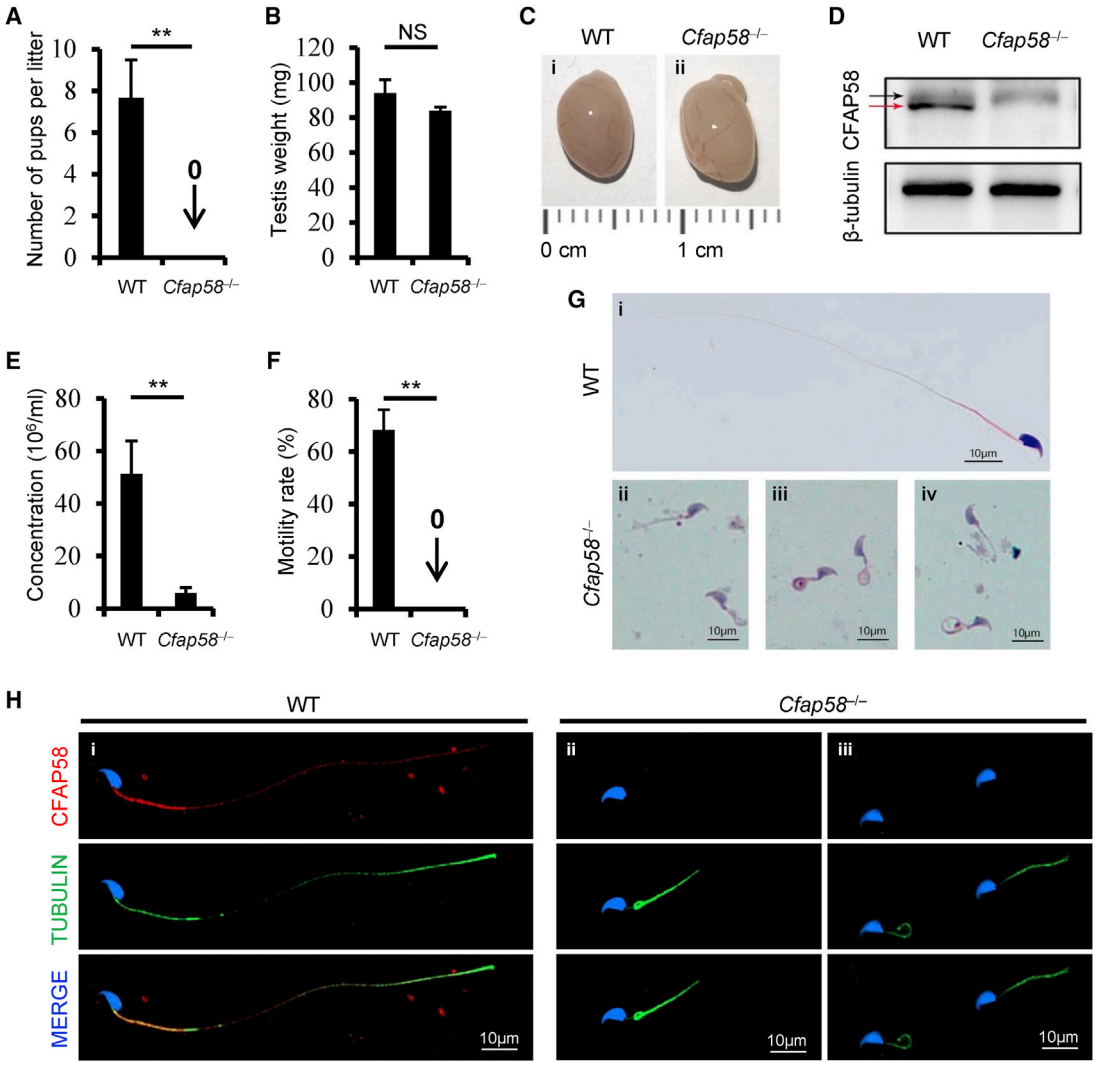

Figure 5. CFAP58 Deficiency Caused Typical MMAF Phenotypes and Infertility in Male Mice

(A) The mean number of the pups per litter was 7.66 ± 1.83 in wild-type (WT) male mice, whereas all the four *Cfap58*-KO (*Cfap58*$^{-/-}$) male mice were completely infertile. **$p < 0.01$.

(B and C) The testis weights (B) and sizes (C) were comparable between *Cfap58*$^{-/-}$ and WT male mice. NS, not significant.

(D) Immunoblotting showed that CFAP58 (noted with a red arrow) was absent in the testis of *Cfap58*$^{-/-}$ male mice when compared with that in WT male mice. The band above CFAP58 was a shallow noise band (noted with a black arrow). β-tubulin was used as a loading control.

(E) Sperm concentration (×10^6/mL) of *Cfap58*$^{-/-}$ male mice was significantly lower than that of WT male mice (6.0 ± 2.0 versus 51.33 ± 12.5, respectively; **$p = 0.0017$). Spermatozoa were collected from mouse cauda epididymis for the analyses of sperm concentration, motility, and morphology.

(F) Sperm motility rate in WT male mice was 68.3 ± 7.6%, whereas the motility dropped to 0 for *Cfap58*$^{-/-}$ male mice. **$p < 0.01$.

(G) H&E staining was used to investigate sperm morphology. When compared with normal morphology of the sperm in WT male mice (i), the sperm cells from *Cfap58*$^{-/-}$ mouse cauda epididymis manifested aberrant ñagellar morphologies, including short and coiled flagella (ii, iii, and iv), which were consistent with the clinical phenotypes in MMAF-affected men.

(H) CFAP58 localization in the spermatozoa from *Cfap58*$^{-/-}$ and WT male mice by immunofluorescence staining. CFAP58 (red) localized at the entire flagella and predominantly concentrated in the mid-piece of normal sperm flagella (i). In contrast, CFAP58 staining was almost absent in the sperm of *Cfap58*$^{-/-}$ male mice (ii and iii). Tubulin indicated the flagella (green), and the nuclei of spermatozoa were Hoechst labeled (blue). Scale bars: 10 μm.

that CFAP58 could be important for ODF transportation and that its deficiency might result in an abnormal location of ODF2, leading to the disorder of the ODF structure.

In conclusion, we found five men harboring bi-allelic LoF variants of *CFAP58* in a cohort of 90 MMAF-affected Chinese men. The functional evidence from *CFAP58*-associated men and *Cfap58*-KO male mice strongly suggests that CFAP58 plays a vital role in sperm flagellogenesis. CFAP58 deficiency can cause abnormalities in both axonemes and peri-axonemes and lead to asthenoteratozoospermia in humans. This study provides new insights for understanding and counseling of MMAF-affected asthenoteratozoospermia.

Table 3. Sperm Morphology of the Wild-Type and *Cfap58*-KO Male Mice

Sperm Morphology[a]	Wild-Type (n = 3)	*Cfap58*-KO (n = 3)
Absent flagella (%)	0.3 ± 0.6	7.3 ± 1.5*
Short flagella (%)	0.0 ± 0.6	50.7 ± 1.5**
Coiled flagella (%)	3.0 ± 2.7	39.0 ± 3.7**
Bent flagella (%)	7.7 ± 1.5	1.0 ± 1.0**
Irregular caliber (%)	0.0 ± 0.0	2.0 ± 1.0
Normal flagella (%)	86.0 ± 2.7	0.0 ± 0.0**

[a]Data represent the means ± SD. *$p < 0.05$, **$p < 0.01$.

Data and Code Availability

The relevant NCBI accession numbers are as follows: NM_001008723.2 (for the reference sequence of human CFAP58), NP_001008723.1 (for the reference sequence of human CFAP58 protein), and NM_001163267.1 (for the reference sequence of mouse Cfap58).

Supplemental Data

Supplemental Data can be found online at https://doi.org/10.1016/j.ajhg.2020.07.010.

Acknowledgments

We would like to thank the families for participating and supporting this study. We also thank the Center of Cryo-Electron Microscopy at Zhejiang University. This work was supported by the National Natural Science Foundation of China (81971441, 81901541, 81601340, 31625015, 31521003, and 81971374), the Foundation of the Department of Science and Technology of Anhui Province (2017070802D150), the Foundation of the Education Department of Anhui Province (KJ2016A370), Shanghai Medical Center of Key Programs for Female Reproductive Diseases (2017ZZ01016), Shanghai Municipal Science and Technology Major Project (2017SHZDZX01), State Key Laboratory of Reproductive Medicine of China (SKLRM-K202002), and Science and Technology Major Project of Inner Mongolia Autonomous Region of China (zdzx2018065).

Declaration of Interests

The authors declare no competing interests.

Received: April 9, 2020
Accepted: July 15, 2020
Published: August 12, 2020

Web Resources

1000 Genomes Project, https://www.internationalgenome.org/
EMBL-EBI Expression Atlas, https://www.ebi.ac.uk/gxa/home
gnomAD, https://gnomad.broadinstitute.org/
GTEx, https://www.gtexportal.org/
Human Protein Atlas, https://www.proteinatlas.org
NCBI, https://www.ncbi.nlm.nih.gov/
OMIM, https://www.omim.org/
Picard, https://github.com/broadinstitute/picard
PolyPhen-2, http://genetics.bwh.harvard.edu/pph2/
SIFT, https://sift.bii.a-star.edu.sg
UCSC Genome Browser, http://genome.ucsc.edu

References

1. Cocuzza, M., Cocuzza, M.A., Bragais, F.M., and Agarwal, A. (2008). The role of varicocele repair in the new era of assisted reproductive technology. Clinics (São Paulo) *63*, 395–404.
2. Agarwal, A., Mulgund, A., Hamada, A., and Chyatte, M.R. (2015). A unique view on male infertility around the globe. Reprod. Biol. Endocrinol. *13*, 37.
3. Krausz, C., and Riera-Escamilla, A. (2018). Genetics of male infertility. Nat. Rev. Urol. *15*, 369–384.
4. Ben Khelifa, M., Coutton, C., Zouari, R., Karaouzène, T., Rendu, J., Bidart, M., Yassine, S., Pierre, V., Delaroche, J., Hennebicq, S., et al. (2014). Mutations in DNAH1, which encodes an inner arm heavy chain dynein, lead to male infertility from multiple morphological abnormalities of the sperm flagella. Am. J. Hum. Genet. *94*, 95–104.
5. Tang, S., Wang, X., Li, W., Yang, X., Li, Z., Liu, W., Li, C., Zhu, Z., Wang, L., Wang, J., et al. (2017). Biallelic Mutations in CFAP43 and CFAP44 Cause Male Infertility with Multiple Morphological Abnormalities of the Sperm Flagella. Am. J. Hum. Genet. *100*, 854–864.
6. Wu, H., Li, W., He, X., Liu, C., Fang, Y., Zhu, F., Jiang, H., Liu, W., Song, B., Wang, X., et al. (2019). NovelCFAP43 andCFAP44 mutations cause male infertility with multiple morphological abnormalities of the sperm flagella (MMAF). Reprod. Biomed. Online *38*, 769–778.
7. Li, W., Wu, H., Li, F., Tian, S., Kherraf, Z.E., Zhang, J., Ni, X., Lv, M., Liu, C., Tan, Q., et al. (2020). Biallelic mutations in *CFAP65* cause male infertility with multiple morphological abnormalities of the sperm flagella in humans and mice. J. Med. Genet. *57*, 89–95.
8. Auguste, Y., Delague, V., Desvignes, J.P., Longepied, G., Gnisci, A., Besnier, P., Levy, N., Beroud, C., Megarbane, A., Metzler-Guillemain, C., and Mitchell, M.J. (2018). Loss of Calmodulin- and Radial-Spoke-Associated Complex Protein CFAP251 Leads to Immotile Spermatozoa Lacking Mitochondria and Infertility in Men. Am. J. Hum. Genet. *103*, 413–420.
9. Li, W., He, X., Yang, S., Liu, C., Wu, H., Liu, W., Lv, M., Tang, D., Tan, J., Tang, S., et al. (2019). Biallelic mutations of CFAP251 cause sperm flagellar defects and human male infertility. J. Hum. Genet. *64*, 49–54.

10. Whitfield, M., Thomas, L., Bequignon, E., Schmitt, A., Stouvenel, L., Montantin, G., Tissier, S., Duquesnoy, P., Copin, B., Chantot, S., et al. (2019). Mutations in DNAH17, Encoding a Sperm-Specific Axonemal Outer Dynein Arm Heavy Chain, Cause Isolated Male Infertility Due to Asthenozoospermia. Am. J. Hum. Genet. *105*, 198–212.
11. Zhang, B., Ma, H., Khan, T., Ma, A., Li, T., Zhang, H., Gao, J., Zhou, J., Li, Y., Yu, C., et al. (2020). A DNAH17 missense variant causes flagella destabilization and asthenozoospermia. J. Exp. Med. *217*, e20182365.
12. Liu, W., Wu, H., Wang, L., Yang, X., Liu, C., He, X., Li, W., Wang, J., Chen, Y., Wang, H., et al. (2019). Homozygous loss-of-function mutations in FSIP2 cause male infertility with asthenoteratospermia. J. Genet. Genomics *46*, 53–56.
13. Martinez, G., Kherraf, Z.E., Zouari, R., Fourati Ben Mustapha, S., Saut, A., Pernet-Gallay, K., Bertrand, A., Bidart, M., Hograindleur, J.P., Amiri-Yekta, A., et al. (2018). Whole-exome sequencing identifies mutations in FSIP2 as a recurrent cause of multiple morphological abnormalities of the sperm flagella. Hum. Reprod. *33*, 1973–1984.
14. Liu, W., He, X., Yang, S., Zouari, R., Wang, J., Wu, H., Kherraf, Z.E., Liu, C., Coutton, C., Zhao, R., et al. (2019). Bi-allelic Mutations in TTC21A Induce Asthenoteratospermia in Humans and Mice. Am. J. Hum. Genet. *104*, 738–748.
15. Liu, C., He, X., Liu, W., Yang, S., Wang, L., Li, W., Wu, H., Tang, S., Ni, X., Wang, J., et al. (2019). Bi-allelic Mutations in TTC29 Cause Male Subfertility with Asthenoteratospermia in Humans and Mice. Am. J. Hum. Genet. *105*, 1168–1181.
16. Lorès, P., Dacheux, D., Kherraf, Z.E., Nsota Mbango, J.F., Coutton, C., Stouvenel, L., Ialy-Radio, C., Amiri-Yekta, A., Whitfield, M., Schmitt, A., et al. (2019). Mutations in TTC29, Encoding an Evolutionarily Conserved Axonemal Protein, Result in Asthenozoospermia and Male Infertility. Am. J. Hum. Genet. *105*, 1148–1167.
17. He, X., Li, W., Wu, H., Lv, M., Liu, W., Liu, C., Zhu, F., Li, C., Fang, Y., Yang, C., et al. (2019). Novel homozygous *CFAP69* mutations in humans and mice cause severe asthenoteratospermia with multiple morphological abnormalities of the sperm flagella. J. Med. Genet. *56*, 96–103.
18. Dong, F.N., Amiri-Yekta, A., Martinez, G., Saut, A., Tek, J., Stouvenel, L., Lorès, P., Karaouzène, T., Thierry-Mieg, N., Satre, V., et al. (2018). Absence of CFAP69 Causes Male Infertility due to Multiple Morphological Abnormalities of the Flagella in Human and Mouse. Am. J. Hum. Genet. *102*, 636–648.
19. Lv, M., Liu, W., Chi, W., Ni, X., Wang, J., Cheng, H., Li, W.Y., Yang, S., Wu, H., Zhang, J., et al. (2020). Homozygous mutations in *DZIP1* can induce asthenoteratospermia with severe MMAF. J. Med. Genet. *57*, 445–453.
20. Cooper, T.G., Noonan, E., von Eckardstein, S., Auger, J., Baker, H.W., Behre, H.M., Haugen, T.B., Kruger, T., Wang, C., Mbizvo, M.T., and Vogelsong, K.M. (2010). World Health Organization reference values for human semen characteristics. Hum. Reprod. Update *16*, 231–245.
21. Li, H., and Durbin, R. (2009). Fast and accurate short read alignment with Burrows-Wheeler transform. Bioinformatics *25*, 1754–1760.
22. Auger, J., Jouannet, P., and Eustache, F. (2016). Another look at human sperm morphology. Hum. Reprod. *31*, 10–23.
23. Liu, C., Lv, M., He, X., Zhu, Y., Amiri-Yekta, A., Li, W., Wu, H., Kherraf, Z.E., Liu, W., Zhang, J., et al. (2020). Homozygous mutations in *SPEF2* induce multiple morphological abnormalities of the sperm flagella and male infertility. J. Med. Genet. *57*, 31–37.
24. Sironen, A., Kotaja, N., Mulhern, H., Wyatt, T.A., Sisson, J.H., Pavlik, J.A., Miiluniemi, M., Fleming, M.D., and Lee, L. (2011). Loss of SPEF2 function in mice results in spermatogenesis defects and primary ciliary dyskinesia. Biol. Reprod. *85*, 690–701.
25. Carter, A.P., Garbarino, J.E., Wilson-Kubalek, E.M., Shipley, W.E., Cho, C., Milligan, R.A., Vale, R.D., and Gibbons, I.R. (2008). Structure and functional role of dynein's microtubule-binding domain. Science *322*, 1691–1695.
26. Burkhard, P., Stetefeld, J., and Strelkov, S.V. (2001). Coiled coils: a highly versatile protein folding motif. Trends Cell Biol. *11*, 82–88.
27. Tapia Contreras, C., and Hoyer-Fender, S. (2019). CCDC42 Localizes to Manchette, HTCA and Tail and Interacts With ODF1 and ODF2 in the Formation of the Male Germ Cell Cytoskeleton. Front. Cell Dev. Biol. *7*, 151.
28. Pasek, R.C., Malarkey, E., Berbari, N.F., Sharma, N., Kesterson, R.A., Tres, L.L., Kierszenbaum, A.L., and Yoder, B.K. (2016). Coiled-coil domain containing 42 (Ccdc42) is necessary for proper sperm development and male fertility in the mouse. Dev. Biol. *412*, 208–218.
29. Yamaguchi, A., Kaneko, T., Inai, T., and Iida, H. (2014). Molecular cloning and subcellular localization of Tektin2-binding protein 1 (Ccdc 172) in rat spermatozoa. J. Histochem. Cytochem. *62*, 286–297.
30. Panizzi, J.R., Becker-Heck, A., Castleman, V.H., Al-Mutairi, D.A., Liu, Y., Loges, N.T., Pathak, N., Austin-Tse, C., Sheridan, E., Schmidts, M., et al. (2012). CCDC103 mutations cause primary ciliary dyskinesia by disrupting assembly of ciliary dynein arms. Nat. Genet. *44*, 714–719.
31. Austin-Tse, C., Halbritter, J., Zariwala, M.A., Gilberti, R.M., Gee, H.Y., Hellman, N., Pathak, N., Liu, Y., Panizzi, J.R., Patel-King, R.S., et al. (2013). Zebrafish Ciliopathy Screen Plus Human Mutational Analysis Identifies C21orf59 and CCDC65 Defects as Causing Primary Ciliary Dyskinesia. Am. J. Hum. Genet. *93*, 672–686.
32. Inaba, K. (2007). Molecular basis of sperm flagellar axonemes: structural and evolutionary aspects. Ann. N Y Acad. Sci. *1101*, 506–526.
33. Inaba, K. (2011). Sperm flagella: comparative and phylogenetic perspectives of protein components. Mol. Hum. Reprod. *17*, 524–538.
34. Eddy, E.M., Toshimori, K., and O'Brien, D.A. (2003). Fibrous sheath of mammalian spermatozoa. Microsc. Res. Tech. *61*, 103–115.
35. Escalier, D. (2003). New insights into the assembly of the periaxonemal structures in mammalian spermatozoa. Biol. Reprod. *69*, 373–378.
36. Wang, W.L., Tu, C.F., and Tan, Y.Q. (2020). Insight on multiple morphological abnormalities of sperm flagella in male infertility: what is new? Asian J. Androl. *22*, 236–245.
37. Neilson, L.I., Schneider, P.A., Van Deerlin, P.G., Kiriakidou, M., Driscoll, D.A., Pellegrini, M.C., Millinder, S., Yamamoto, K.K., French, C.K., and Strauss, J.F., 3rd. (1999). cDNA cloning and characterization of a human sperm antigen (SPAG6) with homology to the product of the Chlamydomonas PF16 locus. Genomics *60*, 272–280.

38. Zhang, Z., Tang, W., Zhou, R., Shen, X., Wei, Z., Patel, A.M., Povlishock, J.T., Bennett, J., and Strauss, J.F., 3rd. (2007). Accelerated mortality from hydrocephalus and pneumonia in mice with a combined deficiency of SPAG6 and SPAG16L reveals a functional interrelationship between the two central apparatus proteins. Cell Motil. Cytoskeleton *64*, 360–376.
39. Sironen, A., Hansen, J., Thomsen, B., Andersson, M., Vilkki, J., Toppari, J., and Kotaja, N. (2010). Expression of SPEF2 during mouse spermatogenesis and identification of IFT20 as an interacting protein. Biol. Reprod. *82*, 580–590.
40. Olson, G.E., and Winfrey, V.P. (1990). Mitochondria-cytoskeleton interactions in the sperm midpiece. J. Struct. Biol. *103*, 13–22.
41. Olson, G.E., and Winfrey, V.P. (1992). Structural organization of surface domains of sperm mitochondria. Mol. Reprod. Dev. *33*, 89–98.
42. Li, Z.Z., Zhao, W.L., Wang, G.S., Gu, N.H., and Sun, F. (2020). The novel testicular enrichment protein Cfap58 is required for Notch-associated ciliogenesis. Biosci. Rep. *40*, BSR20192666.
43. Zhao, W., Li, Z., Ping, P., Wang, G., Yuan, X., and Sun, F. (2018). Outer dense fibers stabilize the axoneme to maintain sperm motility. J. Cell. Mol. Med. *22*, 1755–1768.